Journal of Power Sources 245 (2014) 958–966

Contents lists available at ScienceDirect

Journal of Power Sources

journal homepage: www.elsevier.com/locate/jpowsour

Mechanical and thermal characterization of a ceramic/glass composite seal for solid oxide fuel cells

Bodhayan Dev [a], Mark E. Walter [a,*], Gene B. Arkenberg [b], Scott L. Swartz [b]

[a] Department of Mechanical and Aerospace Engineering, The Ohio State University, 201 West 19th Avenue, Scott Laboratory, OH 43210, USA
[b] NexTech Materials Ltd., 404 Enterprise Drive, Lewis Center, OH 43035, USA

HIGHLIGHTS

- Investigation of ceramic/glass composite for high temperature sealing.
- Micro-voids evolve with increased heating and cooling rates.
- An appropriate heating and cooling rate for curing the seals was determined.
- Thermally induced dimensional responses of cycled seals were determined.
- Microstructure and mechanical properties of cycled seals were studied.

ARTICLE INFO

Article history:
Received 22 March 2013
Received in revised form
8 July 2013
Accepted 9 July 2013
Available online 19 July 2013

Keywords:
Solid oxide fuel cells (SOFCs)
Ceramic/glass seals
Binder burnout
Compression loading
Thermally-induced dimensional response

ABSTRACT

Solid oxide fuel cells (SOFCs) require seals that can function in harsh, elevated temperature environments. Comprehensive characterization and understanding of seals is needed for commercially viable SOFCs. The present research focuses on a novel ceramic/glass composite seal that is produced by roller compaction or tape casting of glass and ceramic powders and an organic binder. Upon heat treatment, micro-voids and surface anomalies are formed. Increased heating and cooling rates during the heat treatment resulted in more and larger voids. The first goal of the current research is to suggest an appropriate heating and cooling rate to minimize the formation of microstructural defects. After identifying an appropriate cure cycle, seals were thermally cycled and then characterized with laser dilatometry, X-ray diffraction, and sonic resonance. From these experiments the crystalline phases, thermal expansion, and elastic properties were determined. Subsequently compression testing with an acoustic emission (AE) sensor and post-test microstructural analysis were used to identify the formation of damage. By fully understanding the characteristics of this ceramic/glass composite seal, next generation seals can be fabricated for improved performance.

1. Introduction

With high efficiencies and low emissions, SOFCs have the potential to change the production and distribution of electrical energy. High temperature operation in the 700–850 °C range is necessary for performance and fuel utilization. The selection of materials for SOFCs has always been a challenge due to this high operating temperature regime; in particular, appropriate materials are expensive and long term stability is a significant concern.

Planar SOFC designs require hermetic sealing between each individual cell to avoid intermixing of air–fuel and to avoid any short circuit in the cell [1–3]. Seals need to have long-term stability and not cause degradation of adjacent materials at the elevated temperatures and in the harsh environments typical to SOFC operation. The performance and life time of a seal depend on the degree to which gas flow within the material and at the interface is inhibited. Therefore, failure of seals is the result of cracking/damage within the bulk and gaps or separation of the interface.

The two mainstream methods for sealing in SOFCs are compressive sealing and chemical bonding sealing [4,5]. In compressive sealing a compliant material is sandwiched between two sealing surfaces and is compressed by an externally applied load. The primary advantage of compressive sealing is tolerance to coefficient of thermal expansion (CTE) mismatches. The disadvantages of the compressive sealing method are the lack of materials that are compliant at high temperature, the chemical reactions occurring in the aggressive SOFC environment, and the need for complicated

* Corresponding author. Tel.: +1 614 292 6081; fax: +1 614 292 3163.
E-mail address: walter.80@osu.edu (M.E. Walter).

0378-7753/$ – see front matter © 2013 Elsevier B.V. All rights reserved.
http://dx.doi.org/10.1016/j.jpowsour.2013.07.054

apparatus that provides mechanical loading [6,8]. The bonding seals approach relies on chemical bonding to provide hermetic sealing. The primary advantages of bonding seals are superior chemical stability under reactive atmospheres and not needing an external load frame for effective sealing [7]. The main disadvantages of bonding seals are brittleness at low temperatures which results in susceptibility to CTE mismatch [8] and poor long term durability resulting from softening and crystallization of the glass phases [7,8]. True hermetic sealing is difficult, if not impossible, to achieve in an environment where temperatures can change. For this reason, the proposed approach is focused on a ceramic/glass composites approach with imperfect, but still acceptable, sealing under compressive loading.

Over the past few decades, extensive research has been carried out in selecting an appropriate composition for glass seals for SOFC applications. It is generally accepted that barium or boron-based systems are required in order to mitigate crystallization at these temperatures [8]. Within these types of systems, authors have studied crystallization kinetics [8,10–12,14,15], CTE development [9,16], particle and powder sizes [21,22], and flow and sintering behavior [7,18,19]. The G-18 glass system developed at Pacific Northwest National Laboratory (PNNL) was developed specifically for SOFCs. As such, this system has been uniquely characterized with measurements of thermal expansion [8,17,20,22], crystallization [22], wetting angle [22], microstructural evolution [23], interaction with interconnect and electrolyte materials [22], mechanical properties [20], and bond strength [17]. The G-18 system has also been modified with different compounds to improve contact angle and thermal expansion characteristics [22]. However G-18 was designed for temperatures up to 700 °C, and when above 700 °C, crystalline phases become unstable and the CTE varies with thermal cycling [22,23]. G-18 also reacts with other SOFC components to form porous interfaces that are susceptible to fracture [24].

Rather than using a "pure" glass approach that starts with a single glass that partially crystallizes into a glass–ceramic, the proposed research deals with two-phase ceramic/glass composites. The ceramic/glass composite approach is an emerging method of high temperature sealing. The processing of the seal begins with a high percentage of Al_2O_3 ceramic powder, an organic binder, and glass powder. The powders are either role compacted or tape cast into flat sheets. Binder burn-out and consolidation of the glass powder occurs during a heat treatment at 800 °C for 4 h. The resulting microstructures consist of glass particles within a matrix of Al_2O_3 powder. The advantage to this approach is that the alumina provides rigidity that minimizes CTE mismatch issues and allows some degree of resistance against compressive loading. However, the methods and results for determining an appropriate curing cycle have not been studied. Most of the past research had chosen an arbitrary curing cycle without mentioning the actual reason behind selecting it [4,8,13,23].

The current research proposes a rigorous procedure to cure the green seals in an appropriate manner that expedites the initial binder burnout process without compromising the seal performance. The study and identification of an appropriate cure cycle is followed by study of the mechanical response of seals that have been cycled multiple times. Given the need to first establish an appropriately cured seal, this paper is organized into four main sections: material system, seal cure, cycled seal characterization, and cycled seal results and discussion.

2. Material system

NexTech Materials, Ltd. employs a novel sealing approach of combining mechanical loading with minimum surface bonding to attain the desired seal performance for SOFCs. The seal itself has a ceramic to glass ratio of 60:40, and is processed by either roll compaction or tape casting of nominally 14 μm glass and 0.5 μm ceramic (alumina) powders mixed with a proprietary binder system developed at Ragan Technologies Inc. (RTI). The glass powders used in the composite seal are a commercial product of Viox and have the trade name "V-1716". The glass composition is the G-18 system invented by Pacific Northwest National Laboratory. G-18 is a barium calcium aluminosilicate-based glass containing the following weight percent mixture of oxides: 35% BaO, 35% SiO_2, 5% Al_2O_3, 15% CaO, and 10% B_2O_3 [28]. The glass transition temperature and melting point of the aforementioned glass have been estimated to be around 620 and 940 °C respectively [7,22]. A typical seal thickness for actual stacks is ~0.25 mm. The glass and alumina phases are shown in the SEM backscatter image provided in Fig. 1.

Thermogravimetric analysis (TGA) was performed on the green seals heated at 2 and 15 °C per minute until 800 °C. TGA was performed to characterize binder burnout and study the effect of different heating rates on binder burnout. As observed in Fig. 2, the seals start to lose weight around 100 °C. The difference in the response curve for 2 and 15 °C heating rates is due to non-uniform temperature distribution within the seal heated at the faster rate. The sudden changes in the slope of the response curve can be attributed to the evaporation or volatilization of different organics in the binder [29,30]. The other phases of the ceramic/glass seal do not volatilize. The TGA curves level out at slightly different temperatures, indicating that the binder burnout is dependent on heating rate. However, since there is no longer measurable weight loss at temperatures above approximately 600 °C and heating of all samples went above 600 °C, it is assumed that binder burnout is complete for all heating rates.

3. Seal cure

The curing process in the present research includes a heating cycle, followed by a 4 h dwell period, and finally a cooling cycle back to room temperature. Smeacetto et al. [3] and Brochu et al. [27] postulated that micro-voids can originate during the curing process primarily due to entrapment of unwanted gases, binder burnout, and also due to differences in the CTE of glassy and ceramic phases. Void formation would be detrimental to the quality of the seal and negatively impact the mechanical response of the seal. The authors are unaware of studies which have investigated void formation as a function of heating or cooling rate.

To expedite the initial curing process in seals, a faster heating and cooling cycle is preferred. However, a faster curing process may

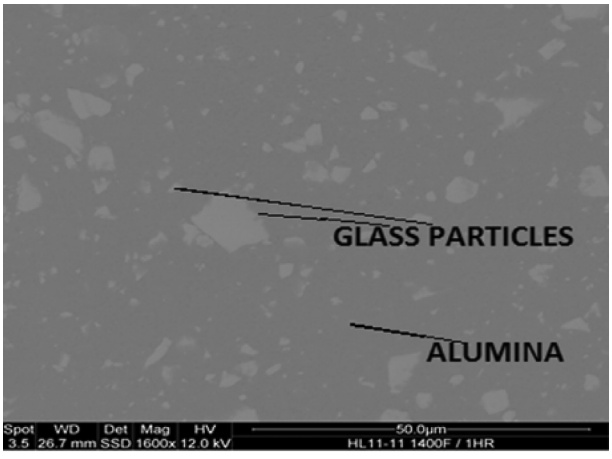

Fig. 1. A backscattered SEM image of a 0.25 mm thick green seal.

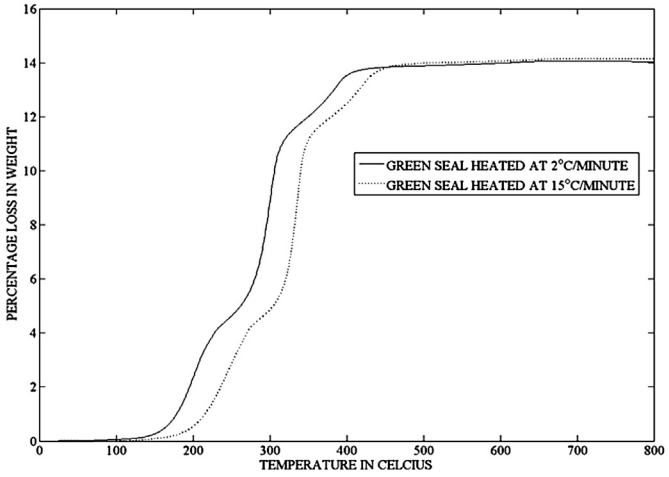

Fig. 2. Thermogravimetric analysis of green seals heated at 2 and 15 °C per minute.

not result in the highest possible seal performance, and it is necessary to investigate if there is an appropriate balance between cure rate and performance. For this purpose, mechanical responses of cured seals were obtained using a compression test. Square specimens having a cross sectional area of 12 × 12 mm^2 and thickness of 1 mm were cut with a razor blade from roll compacted green sheet. To determine the influence of the thermal cure cycle on the mechanical response, specimens were cured with different heating and cooling rates and then subjected to compression experiments.

Compression experiments were performed at room temperature up to a nominal load of 25 N. This level of loading of the current seal samples is equivalent to a mechanical pressure of 0.16 MPa, which is what future stacks could be loaded to. Load and cross-head displacement were recorded throughout the displacement-controlled experiments. Loads and displacements were converted to engineering stress and strain; based on analysis of the load train compliance without specimens, the strains calculated from cross-head displacement were determine to be accurate. The experiments were performed under 0.001 mm s^{-1} displacement control and the data was smoothed to eliminate effects of small steps in displacement associated with low loading rate. After obtaining the mechanical response of each seal, the mechanical response, percentage of voids, and percentage of surface anomalies were correlated. Based on the above analysis, the appropriate thermal cycle for curing the seal is considered to be the one that results in lower percentages of voids and fewer surface anomalies. A lower compressive stiffness is indicative of undesirable micro voids and surface anomalies.

3.1. Heating rate

Green seals were initially heated at rates of 0.5, 2, 5 10, 15, 20, and 25 °C per minute until 800 °C, followed by a constant dwell period of 4 h, and finally they were cooled to room temperature at the respective heating rate. Fig. 3 shows the stress–strain curves of seals cured at different conditions. Although only one experimental curve per sample is shown, the results were highly repeatable. As seen in Fig. 3, the seals heated at rates of 15, 20, and 25 °C per minute experienced sudden load drops prior to reaching the maximum load. The aforementioned seals were crushed to several pieces at the completion of the compression test. The seals cured at 5 and 10 °C per minute did not fail but their compressive stiffnesses were lower than those cured at 0.5 and 2 °C per minute. To further distinguish the 0.5, 2, 5, and 10 °C per minute seals, microstructural analysis was necessary.

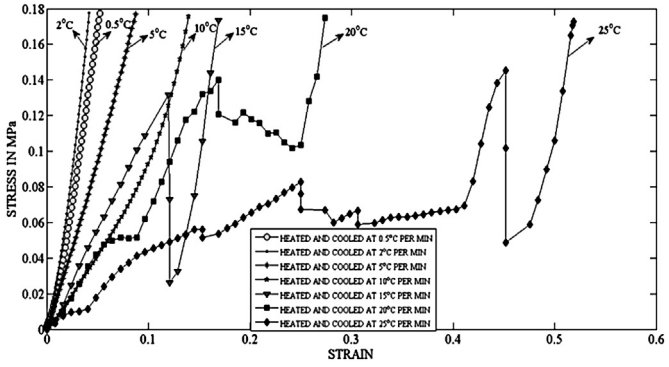

Fig. 3. Stress versus strain curves of seals cured at different heating rates.

As a next step, voids in the SEM images were manually identified. MATLAB® was then used to threshold the images and determine void percentages, thus providing an estimate of the evolution of micro-voids with increased heating rates. For each condition, the SEM images and the corresponding processed images are provided in Fig. 4. In each processed image, the white areas indicate micro-voids. The percentages of micro-voids are presented graphically in Fig. 5. Experiments with 3 and 4 °C per minute heating and cooling were also performed, and although the post-cure stress–strain curves and microstructural images are not presented, the micro-void percentages are included with the other heating rates in Fig. 5. Seals cured at 25 °C per minute have the maximum percentage (24.2%) of micro-voids, and heating rates of 0.5 and 2 °C per minute have the lowest, and nearly identical, percent micro-voids. Even though the 20 and 25 °C per minute heating rates are beyond the range of TGA experiments, since the specimens were cured to 800 °C, it is assumed that complete binder burnout has occurred. However, the binder burnout being a rate dependent process can cause non-uniform temperature gradients within the composite seal system. This behavior can also lead to an increase in the micro-void percentages with a faster heating rate.

It was immediately obvious that seals cured at different heating rates also had different surface features. Surface anomalies like bulges, dimples, and undulations are believed to be generated due to the entrapment of residual gases, inherent manufacturing defects, and flaws [26], and, in actual applications, would result in leak paths at the interface. The surface topography of each cured seal was studied using a stereo optical microscope images and the same image processing approach described in the previous paragraph. Fig. 6 presents the percentage evolution of surface anomalies with increasing heating rate. From Fig. 7 it is clear that 2 °C per minute presents a threshold, above which surface anomalies are occurring.

It is observed from Figs. 3, 4, and 6 that there is a strong correlation between mechanical responses and amount of micro-voids and surface anomalies in seals. The higher percentage of micro-voids and surface anomalies leads to weaker seals. The 0.5 and 2 °C per minute seals have the highest stiffness and a very similar stress–strain response. In addition, the seals cured at 0.5 and 2 °C per minute had essentially the same percentages of micro-voids and no surface anomalies. Hence, in order to expedite the initial curing process without having poor mechanical response, a heating rate of 2 °C per minute was chosen.

3.2. Cooling rate

Now that an appropriate heating rate has been chosen it remains to be seen how cooling rate influences the microstructure and mechanical response. For determining an appropriate cooling

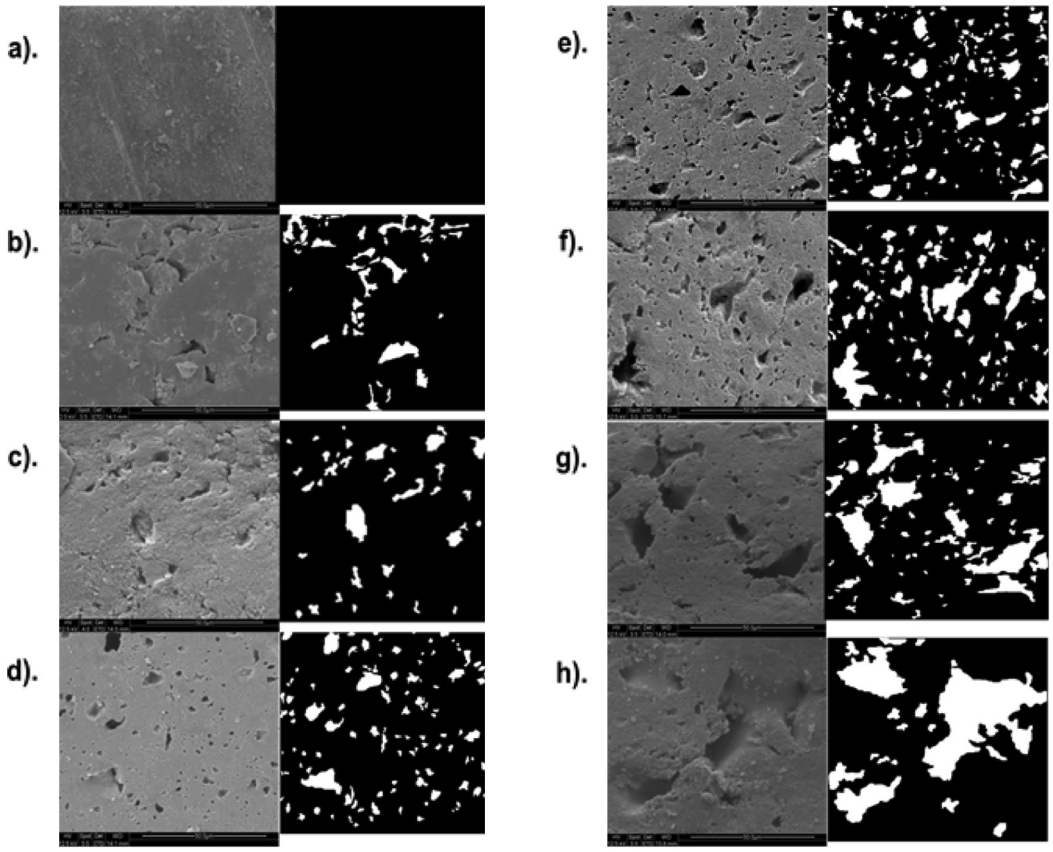

Fig. 4. Cross sectional SEM and processed images of a) green seal, b) cured at 0.5 °C, c) cured at 2 °C, d) cured at 5 °C, e) cured at 10 °C, f) cured at 15 °C, g) cured at 20 °C, and h) cured at 25 °C per minute.

rate, seals were cured at 2 °C per minute, held for 4 h at 800 °C, and then cooled at 2, 5, 10, or 15 °C per minute. It was observed that the formation of surface anomalies depended only on the heating rate, not the cooling rate. Though the current seals were free from surface anomalies, the distribution of micro-voids varied with different cooling rates as shown in Fig. 8. The percentages of micro-voids for the 4 different cooling rates were 7.48, 7.45, 15.6, and 17.3%, respectively. The seal cooled at 2 °C per minute was the same sample used in the determination of appropriate heating rate. It is seen that the seals cooled at 2 and 5 °C per minute have developed nearly the same percentage of micro-voids and are consistent with the heat rate studies.

Fig. 9 shows that the compressive stiffnesses of seals cooled at 2 and 5 °C per minute are nearly identical, and it was observed that they did not fail during the experiment. However, seals cooled at 10 and 15 °C per minute showed spontaneous load drops before reaching the maximum load. These drops are an indication of failure and the specimens were found to be in multiple pieces after the experiment. As there were no significant differences in mechanical responses and microstructures of seals cooled at 2 and 5 °C per minute, to expedite the initial curing process, a cooling rate of 5 °C per minute was chosen. Thus an appropriate thermal cycle for curing the green seal, consists of a heating rate of 2 °C per minute, dwell period of 4 h, and a cooling rate of 5 °C per minute.

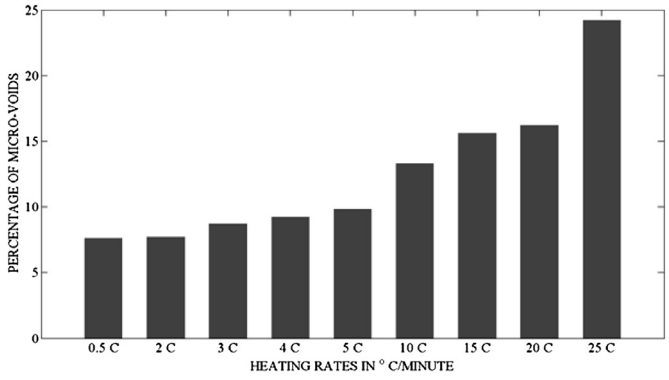

Fig. 5. Variation in percentage of voids for different heating rates.

3.3. Dwell temperature

The current seal material is expected to be used in SOFCs operating at or close to 800 °C. To investigate the microstructural effects of a lower cure temperature, several samples were heated and cooled as described above but were then held for 4 h at only 600 or 700 °C. It was observed that void formation was significantly reduced at these lower temperatures. The compressive stiffnesses of these samples were also higher than all other samples. These results indicated there is a fundamental change in the microstructure between 700 and 800 °C. Since binder burnout process is assumed to be complete before 700 °C, the rate dependent void formation is more likely associated with crystallization.

4. Characterization of cycled seals

It is desirable for SOFCs seals to remain fully functional after multiple heat-up, dwell, and cool-down cycles. Thus it is essential to characterize seals undergoing multiple thermal cycles. This

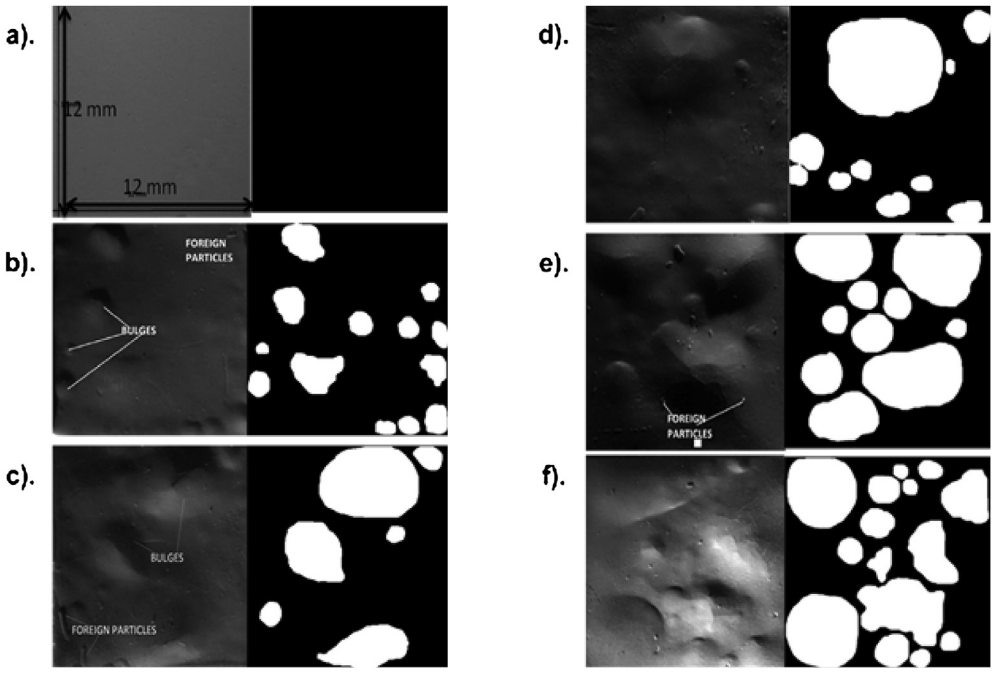

Fig. 6. Stereo optical and processed images of a) cured at 2 °C, b) cured at 5 °C, c) cured at 10 °C, d) cured at 15 °C, e) cured at 20 °C, f) cured at 25 °C per minute.

section presents methods for analyzing dimensional changes, crystallization, elastic properties, and damage.

4.1. Laser dilatometry and XRD for dimensional and phase-change analysis

During thermal cycling, thermal expansion and contraction, glass transition, softening, and crystallization all result in dimensional changes to the seal. It is important to study the dimensional changes associate with all thermo-physical behaviors in order to evaluate the overall performance of the seal. Much of the existing published research focuses only on thermal expansion [8,11,12,17] and not on thermal contraction. The laser dilatometer facility consists of a Centorr high temperature vacuum furnace, a laser source and receiver from BETA LaserMike, and associated data reduction software. The laser source produces a laser sheet that is directed through the furnace. Cylindrical samples are placed in furnace and the interrupted laser sheet is monitored continuously by the receiver. This technique is particularly useful for materials that cannot be contacted, especially those undergoing curing or sintering.

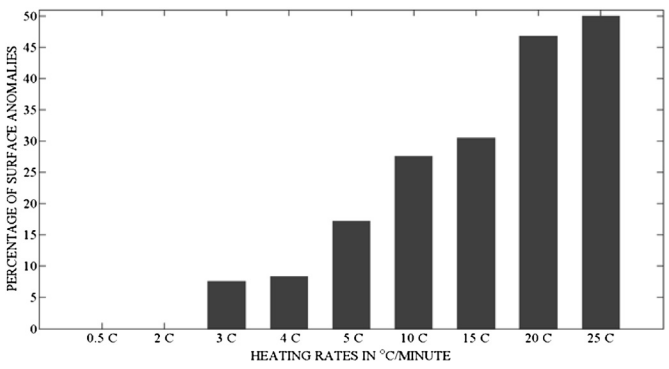

Fig. 7. Variation in percentage of surface anomalies formed for different heating rates.

The laser dilatometry sample consisted of a 16 mm diameter cylinder punched from 2.67 mm thick roll compacted sheet that has same composition described in the previous section. The cylindrical sample was initially subjected to a heat treatment of 4 h at 500 °C. This step was to remove organic binders that might damage the heating elements in the vacuum furnace. The sample was next subjected to the previously identified cure cycle in the laser dilatometer furnace and continuous, temperature dependent dimensional data was obtained. After the first cycle, the seal was subjected to three additional cure cycles in a regular box furnace. The 5th cycle was again monitored with the laser dilatometer. This procedure was repeated so that the 10th cycle was again monitored in the vacuum furnace to obtain the dimensional response. For the cycling in the box furnace, the sample was furnace-cooled to approximately 150 °C between cycles and then immediately reheated for the next cycle. The coefficient of thermal expansion (CTE) in the linear expansion region was calculated based on a linear fit of the data to 550 °C. The softening temperature could be identified by a distinct transition in the laser dilatometer data.

To verify the evolution of crystalline phases in seals with cycled multiple times, X-ray Diffraction (XRD) techniques were employed with a Rigaku Ultima III multipurpose X-ray diffraction system. Samples subjected to 1, 5 and 10 cycles were crushed to approximately 10 μm sized powder. Scans for $5 < 2\theta < 60^{\circ}$ took approximately 4 h and 30 min. The parent elements present in G-18 [28] were used as inputs for analysis of the XRD data.

4.2. Sonic resonance for elastic properties

Elastic moduli of cured seals were determined via a non-destructive sonic resonance technique [25]. This technique identifies the resonant flexural and torsional frequencies of rectangular bar specimens. The resonant frequencies are used to determine the Young's modulus and shear modulus. Elastic moduli of seals cured for 1 and 5 cure cycles were determined from room temperature up to 800 °C.

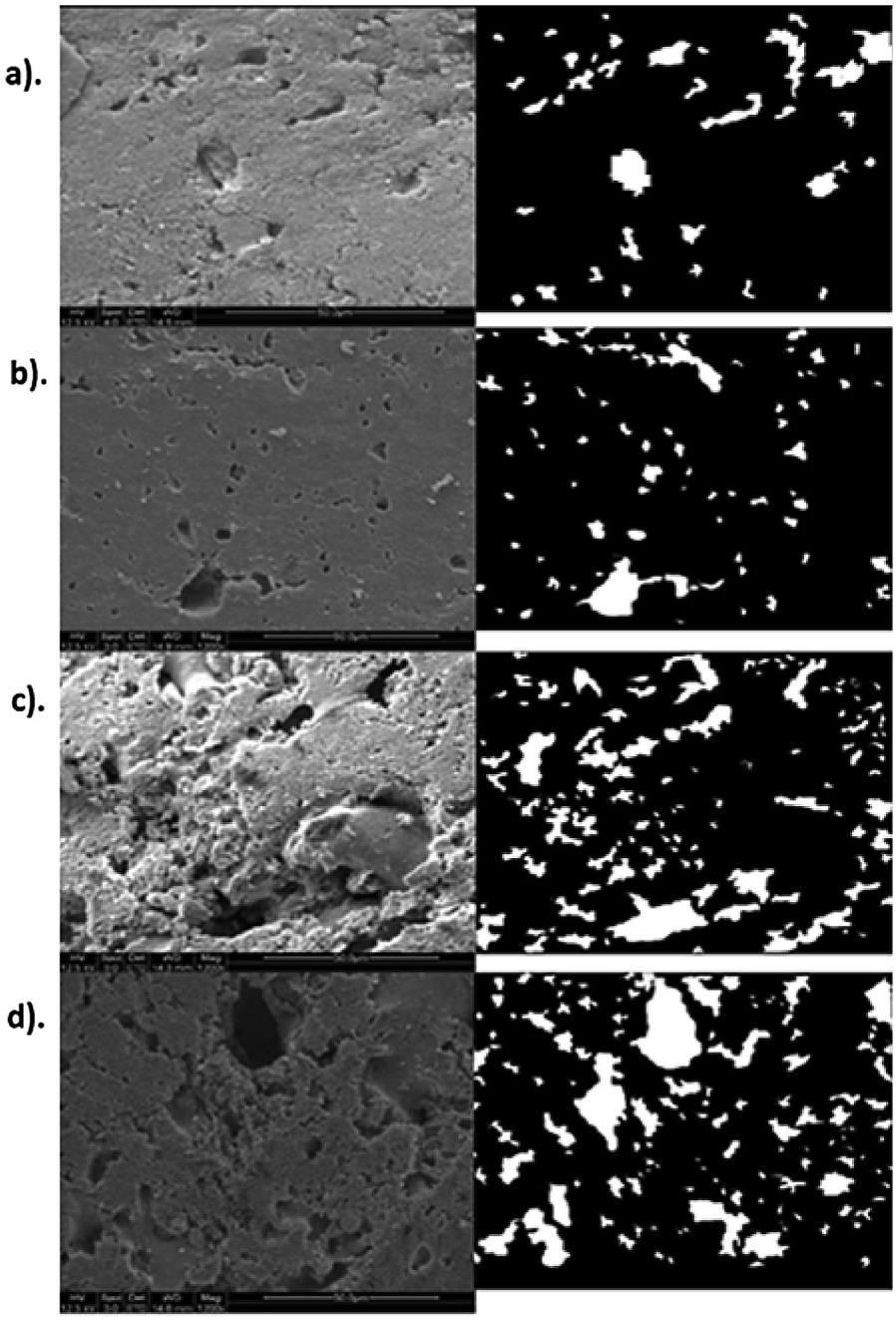

Fig. 8. Cross sectional SEM and processed images of seals a) cooled at 2 °C, b) cooled at 5 °C, c) cooled at 10 °C, and d) Cooled at 15 °C per minute.

4.3. Compression experiments monitored with an AE sensor

With void forming primarily in the 700–800 °C, it is expected that micro-voids continue to form with cycling of the seal material. The evolution and influence of micro-voids were investigated by analyzing the damage developed during room temperature compression experiments. To monitor damage formation, an AE sensor was coupled to the bottom compression platen of the load frame. The AE sensor detects transient surface waves generated from cracking and other deformation phenomenon that release strain energy. After the AE signal was pre-amplified by 34 dB, the signal threshold was set to 40 dB to eliminate unwanted noise from the load frame and test environment. The current compression experiments with AE used seals that were cured at 800 °C for 1 and 5 cycles. Mechanical responses were correlated with percentage of micro voids and synchronized AE patterns.

5. Results and discussion of cycling seals

5.1. Thermally-induced dimensional response and phase evolution

Fig. 10 shows that the thermal response is different for each of the 1, 5, and 10 cycle runs. For the first run, the sample is partially cured, as it has only undergone binder burnout at 500 °C for 4 h. The initial dimensional response is linear, indicating simple thermal expansion of the different constituents. The slope change at 510 °C is believed to be related to the glass

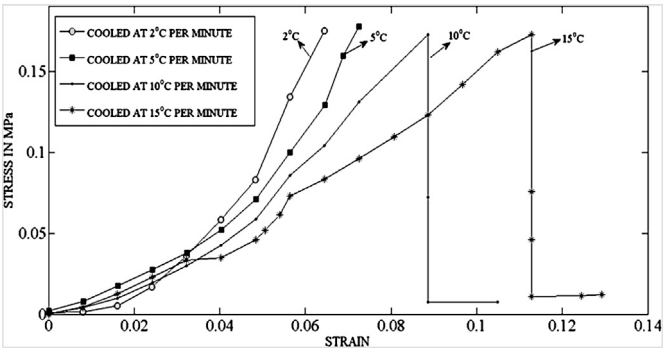

Fig. 9. Stress versus strain curves of seals cured at a heating rate of 2 °C per minute but with different cooling rates.

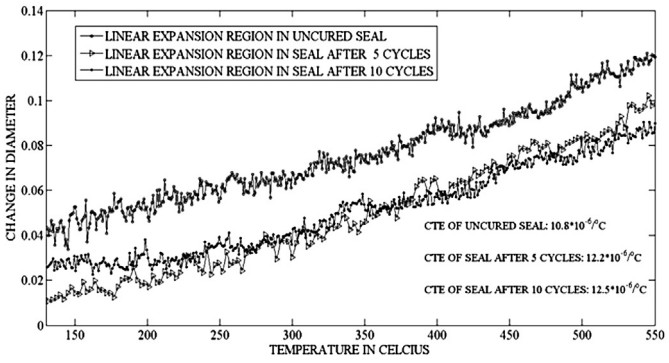

Fig. 11. Linear response of the cycled seals for determining CTE changes.

transition temperature [8,11,17] or in other words, is from the volume change associated with the glass' transition to a viscous fluid. This is a surprising result since the glass transition of G-18 has been reported to be just over 600 °C [22]. The transition in the current data at just over 500 °C is present in both the 1 and 5 cycle data. This variation in the glass transition temperature is assumed to be the effect of alumina powders in green composite seals. At 720 °C, the specimen begins to contract even with increasing temperature. This points to the occurrence of significant microstructural evolution, most likely from the flow of glass into the alumina powder and from crystallization. During the dwell period, the sample continues to contract. Contraction continues in a linear fashion during the cooling portion of the cycle.

As long as there is remaining glassy phase in the sample, additional irreversible crystallization is expected to occur during subsequent cycles. As shown in Fig. 10, the dimensional response of specimen during the 1st cycle is different from that of the 5th. In turn, the 5th cycle is different from the 10th. Although laser dilatometry has not been performed on specimens cycled more than 10 times, since the 10th cycle response is linear during both heating and cooling, it is expected that additional cycling would not lead to a different dimensional response. In Fig. 11, the linear expansion region in each run has been plotted separately to illustrate the variation of CTE for different numbers of cycles. The CTE in the first cycle is calculated as 10.8×10^{-6} °C^{-1}. The CTE changed to 12.2×10^{-6} °C^{-1} and 12.5×10^{-6} °C^{-1} in the 5th and 10th cycles, respectively.

Fig. 12 presents the XRD pattern and crystalline phases of seals cured for 1, 5 and 10 cycles. It is seen that the dominant the peaks formed in cycled composite seals are corundum (Al_2O_3), barium calcium silicate ($Ba_{1.5}Ca_{0.5}SiO_4$), barium aluminum silicate ($BaAl_2Si_2O_8$), barium aluminum oxide ($Al_2Ba_5O_8$), and barium silicate ($BaSiO_3$). The dominant crystalline peaks in a pure G-18 glass are $BaSiO_3$, $BaAl_2Si_2O_8$ and $Ba_{1.5}Ca_{0.5}SiO_4$ [7,22,23]. Additional crystalline phases in the composite seal can be attributed to the inclusion of alumina powders in the starting composition. It is also observed from Fig. 12 that the percentages of crystalline phases increase with increasing number of cycles. As discussed in the previous paragraph, the thermal expansion and contraction of the sample cycled 10 times is linear for the entire temperature range. It is therefore assumed that the 10 cycle sample is fully crystallized.

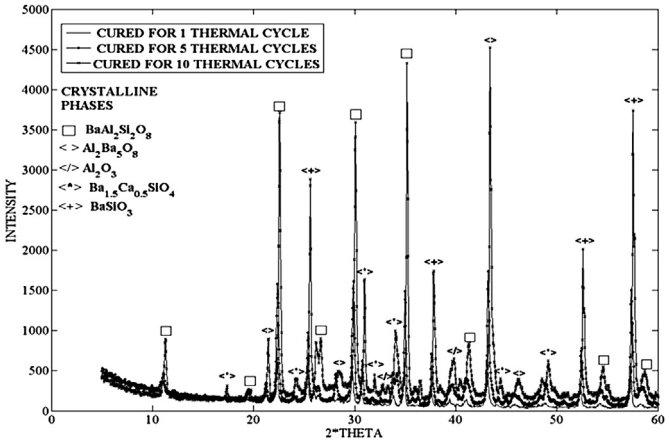

Fig. 12. X-ray diffraction patterns and crystalline phases from seals cured at 800 °C for 1 cycle, 5 cycles, and 10 cycles.

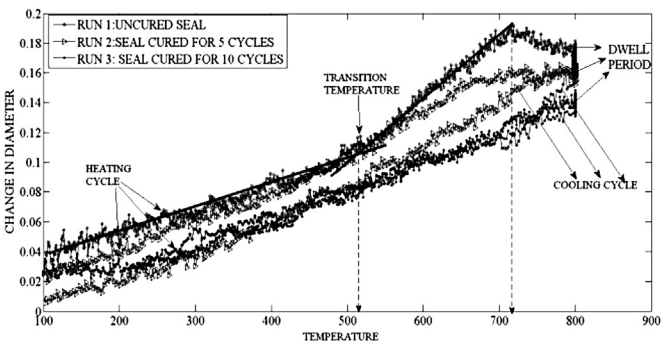

Fig. 10. Variation of thermally induced dimensional response of a seal cycled multiple times.

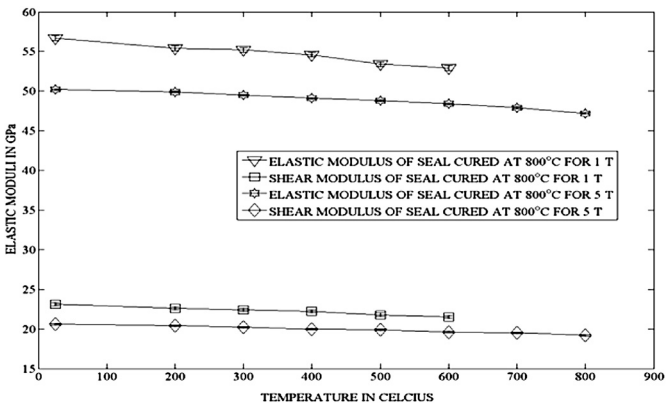

Fig. 13. Temperature dependent elastic moduli for seals cycled 1 and 5 times.

5.2. Temperature dependent elastic moduli for cycled seals

Fig. 13 shows the elastic moduli for seals cured at 800 °C for 1 and 5 cycles. As is consistent with most structural materials, the moduli decreased slightly with increasing temperature. For the 1 cycle seal, it was not possible to distinguish between the first resonant flexural and torsional frequencies for 700 °C and higher measurements. It is suspected that because the seal contains a high percentage of glass and the glass-transition temperature occurs between 500 and 600 °C, the material is not stiff enough for identification of resonant peaks. This was similar to the results obtained by Liu et al. for G-18 [23]. Thus, the measurement of moduli at 700 and 800 °C is not possible for the seal cured at 800 °C for only 1 thermal cycle. For the seal cured at 800 °C for 5 thermal cycles, it was possible to identify resonant peaks at all temperatures. As discussed in the previous section, the multiple thermal cycles led to crystallization; thus the material was stiff enough for resonance measurements above 700 °C.

5.3. Damage in cycled seals

For each of the 1, 5, and 10 cycled seals, Fig. 14 presents the cross-sectional SEM micrographs, their corresponding processed images, and the percentages of micro-voids. The evolution of micro-voids with multiple cycles was consistent with the increasing amounts of crystallized glass. Thus it is again inferred that crystallization plays the dominant role in development of micro-voids. It is anticipated that formation of micro-voids would lead to greater propagation of damage during compression.

Fig. 15 shows the stress–strain curves of seals cured at 800 °C for 1 and 5 cycles along with synchronized cumulative AE data. The seals were again loaded to a value that is representative of actual stack loading, and neither the 1 nor the 5 cycle seal failed in a

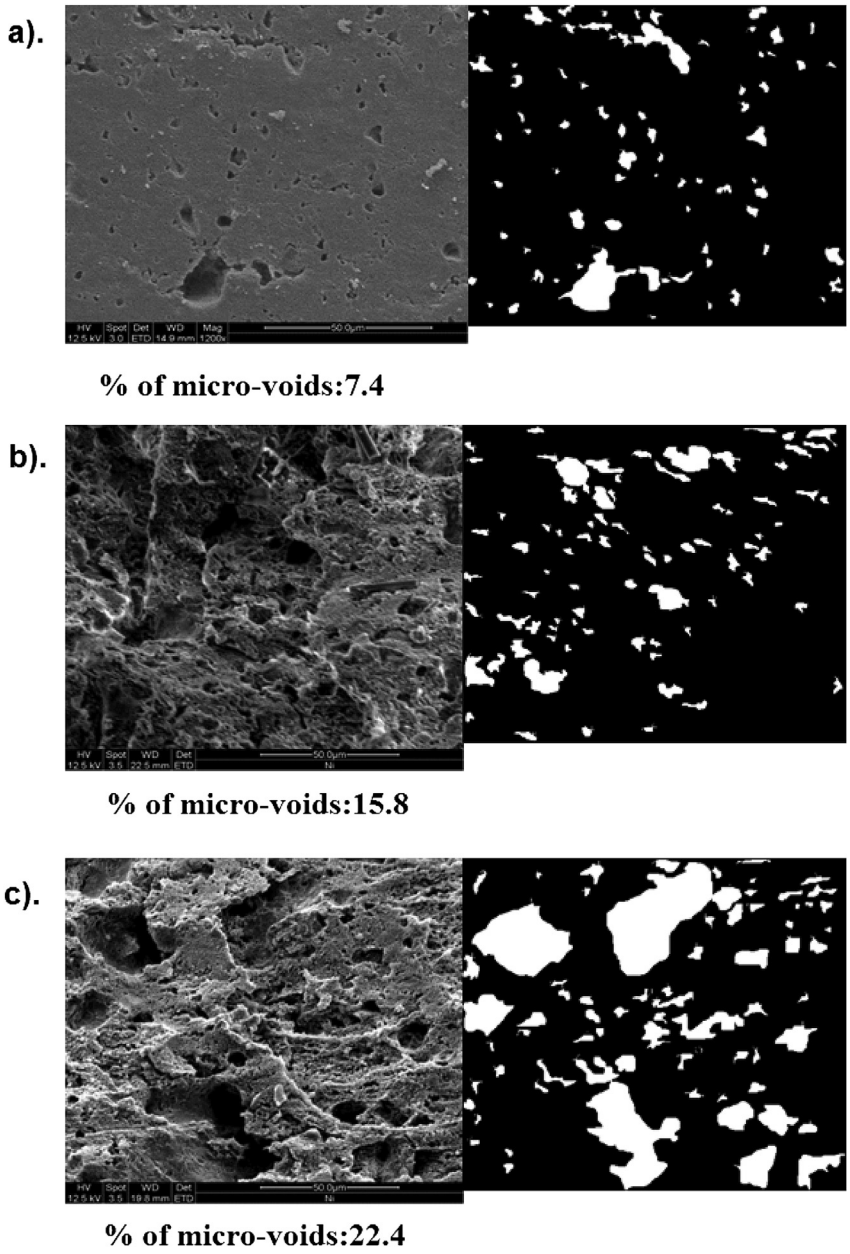

Fig. 14. Cross sectional SEM and processed images of seals a) cured at 800 °C for 1 cycle, b) cured at 800 °C for 5 cycles, and c) cured at 800 °C for 10 cycles.

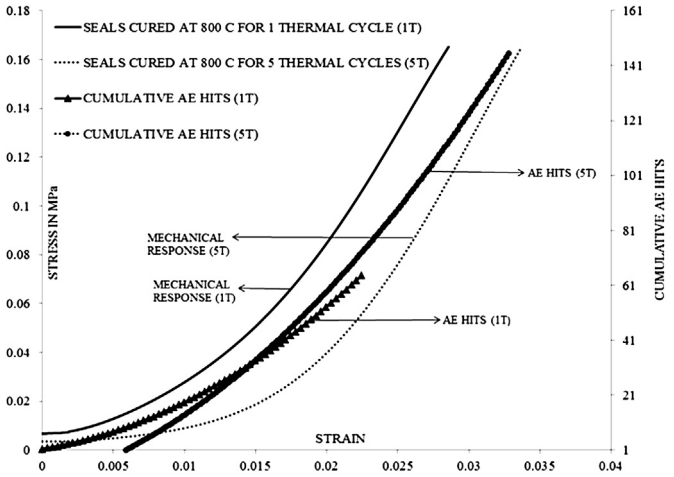

Fig. 15. Stress versus strain curves synchronized with cumulative AE data.

macroscopic manner. However, the seal cured at 800 °C for 5 cycles had lower compressive stiffness and was accompanied by higher AE hits. It is therefore concluded that there is more micro-scale damage during loading in the seal that underwent more cycles. The existence and propagation of more micro-scale damage in the 5 cycle seal is also consistent with microstructural observations and elastic moduli measurements.

6. Summary

This paper has determined an appropriate thermal cycle for curing green, 60:40 ceramic/glass composite seals. The cycle consists of a heating rate of 2 °C per minute, dwell period of 4 h and a cooling rate of 5 °C per minute. This result was based on the study of mechanical responses and SEM micrographs of seals cured at different rates. Thermogravimetric analysis verified that complete binder burnout occurred in the heating process. It was found that voids are formed primarily in the 700–800 °C range and are therefore associated with crystallization. The above methodology for determining an appropriate curing cycle could also be applied to other seal compositions.

The thermally-induced dimensional response of a seal was monitored during the 1st, 5th and 10th cycles. A transition temperature was identified from the initial change of slope during the 1st and 5th cycles. During the 1st cycle, at much higher temperatures the sample began contracting with increasing temperatures. This transition is assumed to be associated with a softening temperature and infiltration of surrounding powder. The responses during the 5th and the 10th cycles were both different from the 1st cycle and from each other. XRD analysis verified the occurrence of progressive crystallization with multiple cycling. The CTE was identified only in the linear expansion zone for each specimen. The CTE differed from the 1st to the 5th cycle due to evolution of crystalline phases. However, the CTE in the 5th and the 10th cycle were nearly identical and close to that of Crofer, a typical interconnect material. Despite the favorable CTE value, crystallization is not beneficial to the current sealing concept that relies on mechanical loading and some degree of compliance.

The seals cured at 800 °C for 1 and 5 cycles had different mechanical properties and damage evolution. Elastic properties were measured with sonic resonance. With higher percentages of micro-voids, the elastic moduli of seals cured for 5 cycles were lower than for the seal cured for 1 cycle. Due to excessive softening at high temperatures, the seal cured for 1 cycle could only be characterized up to 600 °C. The crystallization that occurred on subsequent cycles enabled moduli to be determined for the 5 cycle seals up to 800 °C. Compression experiments with acoustic emission monitoring confirmed that seals cycled 5 times experienced higher levels of damage evolution during loading.

Acknowledgments

This work was supported by the Ohio Department of Development's Third Frontier Fuel Cell Program. The authors would also like to thank the staff of NexTech Materials Ltd. (NTM) for many helpful discussions concerning SOFCs and ceramic/glass composite seals.

References

[1] K.S. Weil, J.E. Deibler, J.S. Hardy, D.S. Kim, G.G. Xia, L.A. Chick, C.A. Coyle, Journal of Materials Engineering and Performance 13 (2004) 316–326.
[2] K. Ley, M. Krumpelt, R. Kumar, J. Meiser, I. Bloom, Journal of Materials Research 11 (1996) 1489–1493.
[3] F. Smeacetto, M. Salvo, M. Ferraris, J. Cho, A.R. Boccaccini, Journal of the European Ceramic Society 28 (2008) 61–68.
[4] Y.S. Chou, J.W. Stevenson, L.A. Chick, Journal of Power Sources 112 (2002) 130–136.
[5] S.P. Simner, J.W. Stevenson, Journal of Power Sources 102 (2001) 310–316.
[6] Y.S. Chou, J.W. Stevenson, Journal of Materials Engineering and Performance 15 (2006) 414–421.
[7] N.P. Bansal, E.A. Gamble, Journal of Power Sources 147 (2005) 107–115.
[8] S. Ghosh, A. Das Sharma, P. Kundu, S. Mahanty, R. Basu, Journal of Non-Crystalline Solids 354 (2008) 4081–4088.
[9] S. Le, K. Sun, N. Zhang, Y. Shao, M. An, Q. Fu, X. Zhu, Journal of Power Sources 168 (2007) 447–452.
[10] N. Lahl, D. Bahadur, K. Singh, L. Singheiser, K. Hilpert, Journal of Electrochemical Society 149 (2002) A607–A614.
[11] J. Tong, M. Han, S.C. Singhal, Y. Gong, Journal of Non-Crystalline Solids 358 (2012) 1038–1043.
[12] A. Arora, K. Singh, O. Pandey, International Journal of Hydrogen Energy 36 (2011) 14948–14955.
[13] M. Solvang, K.A. Nielsen, A.R. Dinesen, P.H. Larsen, in: Proceedings of the IX ECS on Solid Oxide Fuel Cells, vol. 5, 2005, pp. 1914–1931.
[14] M.J. Pascual, C. Lara, A. Duran, European Journal of Glass Science Technology Part B 47 (2006) 572–581.
[15] K. Eichler, G. Solow, P. Otschik, W. Schaffrath, Journal of European Ceramic Society 19 (1999) 1101–1104.
[16] S.B. Sohn, S.Y. Choi, G.H. Kim, H.S. Song, G.D. Kim, Journal of American Ceramic Society 87 (2004) 254–260.
[17] E. Stephens, J. Vetrano, B. Koeppel, Y. Chou, X. Sun, M. Khaleel, Journal of Power Sources 193 (2009) 625–631.
[18] H.T. Chang, C.K. Lin, C.K. Liu, Journal of Power Sources 189 (2009) 1093–1099.
[19] H.T. Chang, C.K. Lin, C.K. Liu, Journal of Power Sources 195 (2010) 3159–3165.
[20] J. Milhans, D.S. Li, M. Khaleel, X. Sun, H. Garmestani, Journal of Power Sources 196 (2011) 3846–3850.
[21] Y. Wang, M. Walter, K. Sabolsky, M. Seabaugh, Solid State Ionics 177 (2006) 1517–1527.
[22] K. Meinhardt, D.S. Kim, Y.S. Chou, K. Weil, Journal of Power Sources 182 (2008) 188–196.
[23] W.N. Liu, X. Sun, M. Khaleel, Journal of Power Sources 196 (2011) 1750–1761.
[24] Z. Yang, K.D. Meinhardt, J.W. Stevenson, Journal of Electrochemical Society 150 (2003) A1095.
[25] Standard Test Method for Dynamic Young's Modulus, Shear Modulus, and Poisson's Ratio by Impulse Excitation of Vibration, ASTM, 2009, p. E1876.
[26] J.C. Glandus, C. Jouin, Journal of Material Science Letters 5 (1986) 503–505.
[27] M. Brochu, B.D. Gauntt, R. Shah, G. Miyake, R.E. Loehman, Journal of the European Ceramic Society 26 (15) (2006) 3307–3313.
[28] K.D. Meinhardt, J.D. Vienna, T.R. Armstrong, L.R. Pederson, U.S. Patent 6,430,966, 2002.
[29] N. Grassie, J.G. Speakman, Journal of Polymer Science Part A-1: Polymer Chemistry 9 (4) (1971) 919–929.
[30] A. Trochimczuk, J. Pielichowski, B.N. Kolarz, European Polymer Journal 26 (9) (1990) 959–961.